International Journal of Applied Engineering Research ISSN 0973-4562 Volume 13, Number 2 (2018) pp. 1014-1034
© Research India Publications. http://www.ripublication.com

Behavior of Different Self-Compacted Concrete Mixes on Short Reinforced Concrete Columns

Dr. Ola Adel Qasim

Doctor, Lecturer, Civil Engineering Department,
Al-Mansour University College, Baghdad, Iraq.

Orcid: 0000-0001-9288-9334

Abstract

Reinforced concrete columns represented the main load bearing members of any type of structure and should be designed adequately since it supports beams and slabs and transfers the load to the foundation. The strength of columns is controlled by the strength of the material used (grade of concrete) and the (cross-section geometry). Plane self-compacted concrete is facing a weakness in cracking resistance, this leads to applying of steel fiber in the concrete mixes, but steel fiber reduced the SCC workability. The opposing effects are the subject of this investigation. This research investigates experimentally and analytically the influence of steel fiber with volume fraction (0, 1 and 2% by volume) on ultimate capacity and the deformation behavior of three types of (normal, high and ultra-high self-compacting concrete) with different compressive strength on reinforced concrete column of size (100*100*700mm) under concentric loading. Nine short reinforced concrete columns are examined and compared. These columns divided into three groups each group contains 3 columns with different steel fiber ratio. Experimental data for strength, deformation, and failure mode were obtained for each test. Properties of hardened SCC were investigated. To determine the workability, different test methods are adopted in this research such as slump flow, T50, and L-box. Results indicated that the properties of different SCC can be improved by the addition of steel fiber. The inclusion of steel fibers was an effective way to prevent spalling of the concrete cover, increase the ductility and increases strength. Finite element (ANSYS software program) is used for the analysis. The analytical results are in high-grade complying with the experimental data. The comparison shows that the ANSYS is capable of modeling and predicting the actual behavior of reinforced concrete column.

Keywords: Column, Steel fiber, SCC, Normal concrete, High-strength concrete and Ultra-High strength concrete.

INTRODUCTION

The structural member (reinforced concrete columns) is used generally to hold and carry axial loads through it. There are many factors effects the ability of columns to carry loads, these factors are; firstly, the grade of concrete (compressive strength) related to the strength of materials and secondly the shape of the section related to the geometry and finally the mechanism of transferring the loads [1, 2]. The concrete named (Self-compacted) is a type of concrete widely used in practice at all over the world for its excellent physical and mechanical properties and the improvement in workability and simplicity of experimental work in sites and represented one of the most outstanding advances in concrete technology. The only lack of deficiency of this type of concrete is the low tensile strength related to the brittle behavior. Self-compacted concrete presented a reduction in structure deformation and whenever concrete with resistant to segregation and bleeding are needed. The new concrete technology in structure constructions and material types are directly demanded the economy concrete, design but at the same time, a stronger material must be applied. Self-compacting concrete (SCC) has the ability to presented a multiple of improved advantages which are, (excellent workability, self-compacting, labor for vibration is excluded, and the extra construction work from vibration, frame works and construction costs can be minimized).

To overcome and improved tensile strength, energy absorption, cracking resistance and ductility, steel fiber must be added [3, 4]. Not only steel fiber has improved the characteristics of SCC concrete but many researchers investigated different types of fillers and its effect on the microstructure of the concrete matrix especially minimizing the interfacial transition zone between the cement paste and the aggregate and reducing the porosity related to pore size distribution which enhanced the compaction [5]. The effect of materials used improved the self-compacted reinforced concrete column and its behavior with many loading types. Many researchers used steel fiber in their experimental work. There are significant differences between different SCC concrete, so this research investigated the mechanical properties and behavior of different self-compacted concrete mixes of short reinforced concrete column. A finite element analysis using ANSYS program was utilized to model the tested columns. The comparison between numerical finite element results and experimental results of the columns presented and discussed.

LITERATURE REVIEW

Many researchers study the self-compacted concrete with different parameters and grade of concrete with variables materials. [Holschemacher and Klug, 2002] presented a comparing study with the differences between normal concrete and self-compacted concrete in term of hardened state properties and fresh properties including compressive, shear, tensile, flexural strength and shrinkage with creep test. [Sonebi, et.al., 2007] an experimental study of the factors affecting on the fresh self-compacting concrete under different variable like; w/c ratio, aggregate size and superplasticizer are presented with

comparison in term of passing, filling ability of concrete. [Grunewald and 2001] presented an experimental work with the comparison between plain and fiber self-compacted concrete. They used 4 types of steel fiber with variables content to study fiber effects on workability. [Suksawang, N. et. al., 2006)] investigated the differences between high performance concrete, self-compacted concrete and normal concrete and in term of hardened state properties and fresh properties with effect of additive materials. The tests show that self-compacted concrete is weak in modulus of elasticity but with higher shrinkage [Ferrara, L., et.al., 2007] investigated the fiber with different type and ratio effect on self-compacted concrete and normal strength properties. [Nehdi and Ladanchnk, 2004] presented an experimental study on the effect of hybrid steel and polymer fibers with different ratios in term of fresh and hardened concrete characteristic. They concluded that fibers increase strength, cracking and toughness and all mechanical properties. [Heba A., 2011] study the effect of silica fume, flyash as additives with different content materials on strength of self-compacted concrete. The conclusions were additive increase compressive strength but reduce the workability. The same results are presented in [Xie Y., et. al., 2002] research. [MuctebaUysal, 2012] effect of high temperature on the self-compacted concrete characteristic is presented in this research with different types of additives materials like; (limestone, basalt and marble powder) with polypropylene fiber. Conclusions are presented were, the increasing of fine powder with higher replacement and high temperature effect reduce compressive strength. [Foster and 2001] Effect of hooked steel fiber on reinforced high strength concrete column is presented under concentric or eccentric loading.

They proved that the inclusion of steel fiber reduces concrete cracking and increased the ductility. [Efe and Musbau 2011] presented an experimental work on the effect of different steel fiber content and shape upon laterized concrete columns. They concluded that there is a relationship between concrete strength and higher ultimate load. [Hadi. M. 2009] this paper included the effect of fiber on high strength concrete of circular reinforced concrete columns. The columns are divided in three types (one with fiber, one without fiber and one with fiber subjected at the outer size). The results show increasing in steel fiber content reduces carking and increase the ultimate load and ductility. [Campion, G., et.al., 2010] presented reinforced concrete confined columns with non-fiber or with fiber normal and high strength concrete with concentric and eccentric loading and effect of fibers on the thickness of columns cover. [Maha, M.S., et. al., 2013] study the effect of reactive powder concrete and higher strength concrete type on behavior of short columns with or without reinforcement.

Detail of the Experimental Program of Concrete Column

The experimental program consists of casting and testing nine short column models of the same dimensions (100*100*700mm) with and without steel fiber with normal, high and ultra-high self-compacting concrete mix to investigate the difference in behavior of these models when subjected to axial loading. The experimental program consists of three group each group has three columns of NSCC, HSCC, and UHSCC were casting and testing with three volume fraction of fiber to compare these column's behavior when subjected to axial loading as shown in Figure (1) and table (1). All columns specimens have a top and bottom bearing rubber hat of 2mm thick plate to prevent end bearing failure of the two ends and to insure that the load is distributed uniformly overall the column ends. All specimens were reinforced with four longitudinal steel bars of 10 mm diameter (with 4-φ10 mm). Ties were made of (φ4mm) bar diameter and spaced at (75mm) in all the specimens and the clear cover was (6mm).

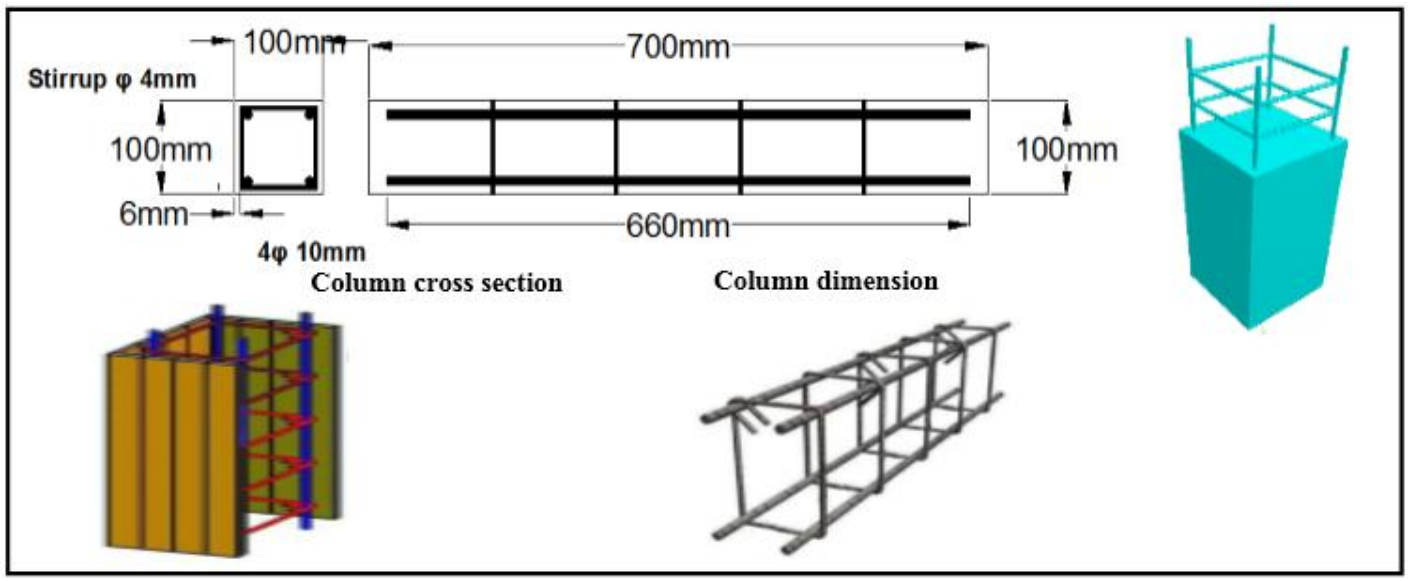

Figure 1: Details dimensions and reinforcement of the tested column.

Table 1: Details of NSCC, HSCC, and UHSCC columns.

Mix	Dimension (mm)	Longitudinal steel bars	Tie bars	Column type
UHSC-SCC	100*100*700	4-φ10	4-φ4	Ultra high strength concrete
UHSC–SCC	100*100*700	4-φ10	4-φ4	
UHSC-SCC	100*100*700	4-φ10	4-φ4	
HS-SC	100*100*700	4-φ10	4-φ4	High strength concrete
HS-SC	100*100*700	4-φ10	4-φ4	
HS-SC	100*100*700	4-φ10	4-φ4	
N-SC	100*100*700	4-φ10	4-φ4	Normal concrete
N-SC	100*100*700	4-φ10	4-φ4	
N-SC	100*100*700	4-φ10	4-φ4	

Description of Materials and Properties

Cement

Type I according to ASTM (OPC) Ordinary Portland cement was applied in all concrete mixture in the experimental work used produced at the Northern cement factory, as shown in Figure (2) which follows the limits and conditions of [IQS specification] and [ASTM C150-89]. Table (2) show the physical and chemical composition of ordinary Portland cement.

Table 2: Physical and chemical composition of ordinary Portland cement.

Composition Percent (%)	Limitations of IQS
[CaO….62], [SiO_2….21], [Al_2O_3….4.5],[Fe_2O_3…..5.0]	---
MgO…..2.28	≤5.0
SO_3…..1.98	≤2.8
L.O.I. …..2.45	≤4.0
I.R. …..0.47	≤1.5
L.S.F. …..0.94	0.66-1.02
[C_3S…..57.3], [C_2S…..16.3], [C_4AF…..13.7]	-
C_3A…..8.5	> 5.0
Fineness (cm^2/gm) …..3329.0	≥2300 cm^2/gm
Soundness (%)…..0.7%	≤0.8
Setting time (hrs: min) ….. Initial 2:10 Final 3:45	[≥ 1:00 >0.45 min]-[≤ 10:00 hrs.]
Compressive Strength (3 and 7 day)(MPa) …..32, 41	[≥ 15 MPa]- [≥ 23 MPa]

Fine Aggregate

Traditional fine sand applied for normal concrete mixes while for high and ultra-high type a fine silica sand known as "glass sand" were used as shown in Figure (2). Fine grading satisfies the [IQS specification]. Table (3) show grading of fine aggregate and table (4) show physical properties of fine aggregate. Figures (3 and 4) shows the grading of aggregates.

Table 3: Grading of fine aggregate.

Sieve Type (mm)	Natural Sand		Silica sand	
	Cumulative Passing %	IQS Limits, (Z. 2)	Cumulative Passing %	IQS Limits (Z.4)
4.75	100	90-100	100	95-100
2.36	85	75-100	100	95-100
1.18	72	55-90	100	90-100
0.60	48	35-59	90	80-100
0.30	23	8-30	25	15-50
0.15	7	0-10	8	0-15

Table 4: Physical properties of fine aggregate.

Physical properties	Limitations of IQS (Z.2)
Specific gravity…(2.1%)	---
Sulfate …(0.076%)	≤0.5%
Absorption…(0.68%)	---

Coarse Aggregate

Coarse aggregate related to [IQS specification] with the maximum particle size of 10mm was applied in the experimental work in normal concrete mixes only. The grading curve of the coarse aggregate is shown in Table (5) and Figure (5). Table (6) shows physical properties of coarse aggregate related to [B.S. limits].

Table 5: Grading of coarse aggregate.

Sieve Size (mm)	Cumulative Passing (%)	Limitations of IQS
10	100	100
4.75	90	85-100
2.36	20	0-25
1.18	0	0-5

Table 6: Physical properties of coarse aggregate.

Physical Properties	Limits of B.S.882/1992 specification
Specific gravity… (2.84%)	---
Sulfate (SO_3) …(0.04 %)	≤ 0.1%
Absorption…(0.54%)	---

Figure 2: Cement, fine and coarse aggregate used.

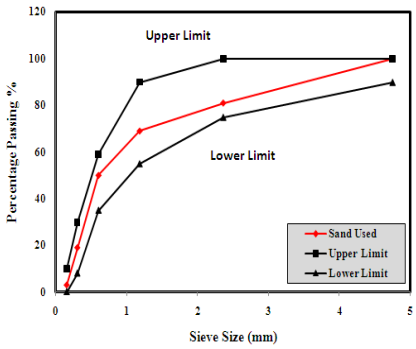

Figure 3: Grading curve for fine aggregate.

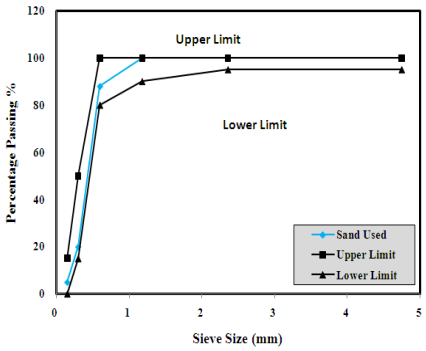

Figure 4: Grading curve for glass sand aggregate.

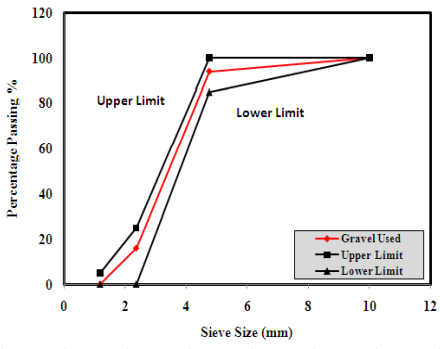

Figure 5: Grading curve for coarse aggregate.

Silica Fume Admixture (SF)

Grey silica fume as a mineral admixture with specific gravity=2.3 and specific surface=20 produced from (Basif Company) has been used complying with [ASTM C1240-04] conditions and requirements as shown in tables (7). It's represented as extremely active pozzolanic substance and produce from the production of silicon material. Silica fume is an extremely fine powder, with the grain size of approximately (100 times) lesser than an average cement particle size as shown in Figure (6).

Table 7: Chemical and physical analysis of the silica fume.

Chemical, Physical properties and Composition	ASTM C 1240 limits
SiO2 or Silicon dioxide (%)……..89	>85.0
Moisture (%)……..0.8	<3.0
Loss of ignition……..2.4	<6.0
% retained on sieve No. 325……6	<10
Activity Index AI……126	>105

Water Reducing Agent (Superplasticizer)

Chemical product with (colorless appearance) or a reducing agent with trade name Sika-ViscoCrete-5930 produce by SIKA company was using her as shown in Figure (6). It works as a superplasticizer, viscosity factor and hardness retarder and all these factors lead to minimize water in mixing and develop compressive, tensile, bending and shear strength as specified in [ASTM C109/C109M-05]. Table (8) indicates the technical description of the superplasticizer used.

Table 8: Technical description.

Properties, Chemical and Description	
Compatibility- Dosage -Flammability	Aqueous product of modified polycarboxylates based polymer. Used with any cement type with a dosage of (1.0 to 2.0%) by weight of binder and (flammable= Non)
Storage	12 months in dry situation at 5-35°C.
Density	About 1.085 kg/l (in 20°C)
Solid Content and Viscosity	(23-27%)-(120-180 MPa at 20°C)
Chloride and PH	(0.1%)-(4)

Steel Fibers

Straight and round steel fibers of length=(13mm), diameter=(0.2mm), Density =(7800 kg/m^3), Modulus of Elasticity=(210 GPa) and Tensile strength=(2600 MPa) complying with [***ASTM A820/A 820M-04***] as shown in Figure (6) was used. In experimental work fibers usually used from (0 up to 2% by volume). An increase in fiber content leading to reduce the concrete workability. Table (9) shows the properties of the used steel fibers.

Table 9: Properties of steel fiber.

Chemical composition (%)
Carbon C=0.7
Silicon Si= 0.2
Manganese Mn=0.5
Phosphorus P=0.03
Sulfur S=0.023
Chromium Cr=0.9
Aluminum Al=0.003

Steel Reinforcement

All specimens were reinforced with four longitudinal steel bars (with 4-φ10 mm.), as shown in Figure (7). Ties were made of 4mm bar diameter and spaced at 75mm in all the specimens and the clear cover was 6mm. Table (10) show properties of steel bars used.

Table 10: Properties of steel reinforcement.

Bar size (mm)	A (mm^2)	f_y (MPa)	f_u (MPa)	E_s (GPa)
4	12.56	517	601	200
10	78.5	611	725	200

Figure 6: Silica fume, superplasticizer and steel fiber used.

Figure 7a: Testing machine.

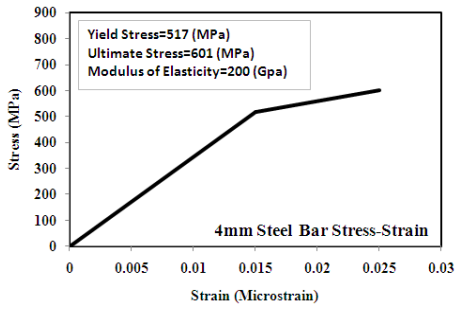

Figure 7b: Tensile stress-strain curves for φ4 mm

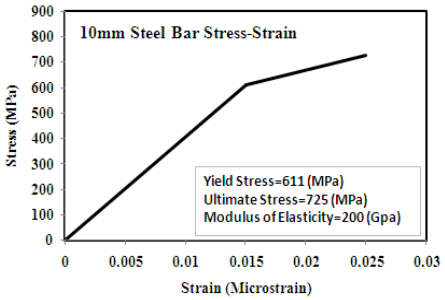

Figure 7c: Tensile stress-strain curves for φ10 mm

Table 11: Details of Mix design for NSCC, HSCC, and UHSCC.

Mix	Cement kg/m^3	Gravel kg/m^3	Sand kg/m^3	additive by weight of cement	Steel fiber by volume	Superplastisizer % by weight of cement	w/c	f'c MPa
UHSC-SCC	1000	0	1000	10%	0%	6.80%	0.17	95
UHSC–SCC	1000	0	1000	10%	1%	6.80%	0.17	115
UHSC-SCC	1000	0	1000	10%	2%	6.80%	0.17	125
HS-SC	547	775	845	10%	0%	4.60%	0.3	50
HS-SC	547	775	845	10%	1%	4.60%	0.3	60
HS-SC	547	775	845	10%	2%	4.60%	0.3	70
N-SC	394	767	770	10%	0%	1.90%	0.477	30
N-SC	394	767	770	10%	1%	1.90%	0.477	35
N-SC	394	767	770	10%	2%	1.90%	0.477	39
volume	100*100*700		0.007 m3					

Table 12: Mix design proportion of SCC and results of fresh concrete properties.

Mix design	Steel fiber V_f %	Slump (mm)	Percentage (%)	T_{50} (sec)	Percentage (%)	L-Box (H2/H1)	Percentage (%)
UHSC-SCC	**0%**	750	0.00	2.1	0.00	0.97	0.00
UHSC–SCC	**1%**	670	-10.67	3.14	49.52	0.88	-9.28
UHSC-SCC	**2%**	580	-22.67	4.5	114.29	0.8	-17.53
HS-SC	**0%**	780	0.00	2.5	0.00	0.98	0.00
HS-SC	**1%**	750	-3.85	2.9	16.00	0.93	-5.10
HS-SC	**2%**	720	-7.69	3.4	36.00	0.88	-10.20
N-SC	**0%**	750	0.00	2.5	0.00	1	0.00
N-SC	**1%**	680	-9.33	3.5	40.00	0.96	-4.00
N-SC	**2%**	650	-13.33	4	60.00	0.92	-8.00
Limit of EFNARC		650-800		2-5		0.8-1	
Limit of ACI-237		450-760		2-5		0.8-1	

Mix Proportions

Three concrete types (normal high and ultra-high strength self-compacted concrete) with different percentage of steel fiber (0, 1.0 and 2.0%) as shown in tables (11) with the proportion of the constituents for the prepared concrete mixes as shown below:

1- For ultra-high strength concrete (1: 1: 0:0.1) (by weight of OPC ordinary Portland cement: F.A fine aggregate: C.A coarse aggregate, Silica fume, with w/c ratio of 0.17).

2- For high strength concrete (1: 1.54: 1.42:0.018) (by weight of OPC ordinary Portland cement: F.A fine aggregate: C.A coarse aggregate, Silica fume, with w/c ratio of 0.3).

3- For Normal strength concrete (1: 1.95: 1.95:0.025) (by weight of OPC ordinary Portland cement: F.A fine aggregate: C.A coarse aggregate, Silica fume, with w/c ratio of 0.477).

Properties of Fresh Concrete

To measure and represents the fresh characteristics of self-compacted concrete there are three tests types, these methods are (the ability of the concrete to flow within the molds and it's all volume sizes depending on weight only. The ability of the concrete to enter and flow through the narrow spaces, which are actually the distances between reinforcing steel or some places required to be poured in small sections without the accumulation of concrete above the section or the separation of concrete. Finally, the capability of the concrete to stay homogenous while mixing, transport and casting of structures.

The current research presents the properties of the concrete in the case of fresh through several tests to ensure the properties of self-compacted concrete mixtures, which follow the required specifications in [EFNARC and ACI-237R07], these tests are (slump flow, T50, and the L-box test) were used for all mixes types. Figure (8) show the fresh SCC test.

- For ultra-high SCC from the table (12) and Figures (9, 10 and 11) that the addition of fibers with 1% and 2% decreases the slump flow by (10.7% and 22.7%), increasing T50 (49.5% and114.3%) reduction L-box by (9.3% and 17.5 %). This reduction of workability is due to the presence of steel fibers that work as the obstacle for the motion of mix components.
- For high SCC from the table (12) and Figures (12, 13 and 14) that the addition of fibers with 1% and 2% decreases the slump flow by (3.8% and 7.7%), increasing T50 (16% and 36%) reduction L-box by (5.1% and 10.2 %). This reduction of workability is due to the presence of steel fibers that work as an obstacle for the motion of mix components.
- For normal SCC from the table (12) and Figures (15, 16 and 17) that the addition of fibers with 1% and 2% decreases the slump flow by (9.3% and 13.3%), increasing T50 (40% and 60%) reduction L-box by (4% and 8%). This reduction of workability is due to the presence of steel fibers that work as an obstacle for the motion of mix components.

Slump flow test

L-box test

V-funnel test

Figure 8: fresh SCC test.

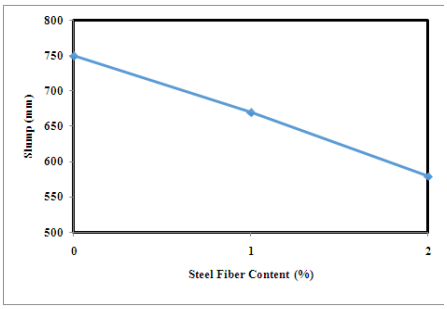

Figure 9: Effect of steel fiber content on slump test (mm) on ultra-high SCC concrete.

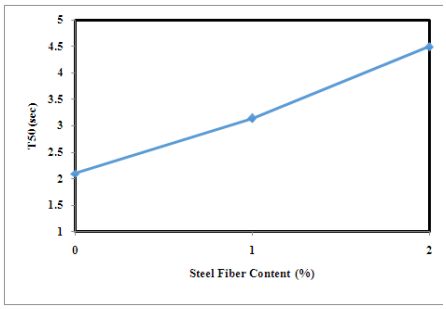

Figure 10: Effect of steel fiber content on T_{50} (sec) on ultra-high SCC concrete.

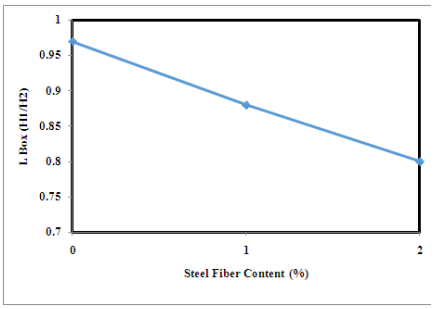

Figure 11: Effect of steel fiber content on L-Box on ultra-high SCC concrete.

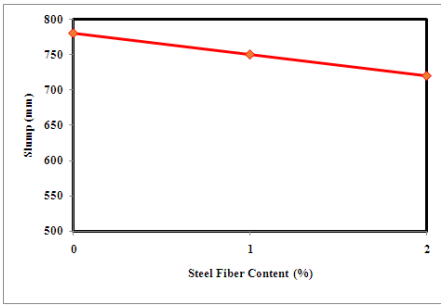

Figure 12: Effect of steel fiber content on slump test (mm) on high SCC concrete.

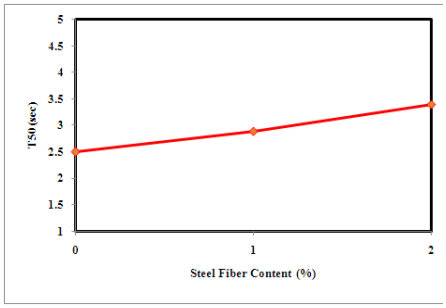

Figure 13: Effect of steel fiber content on T_{50} (sec) on high SCC concrete.

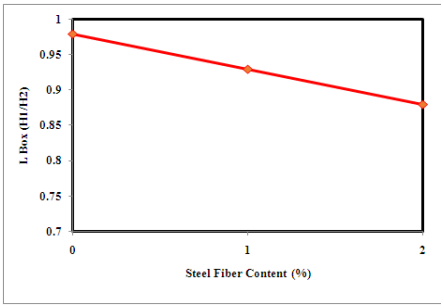

Figure 14: Effect of steel fiber content on L-Box on high SCC concrete.

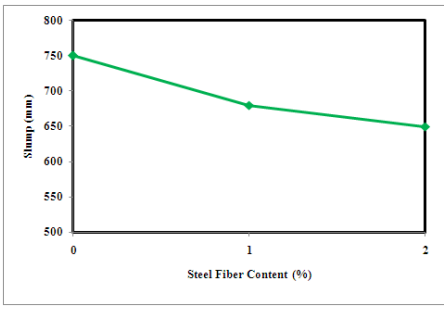

Figure 15: Effect of steel fiber content on slump test (mm) on normal SCC concrete.

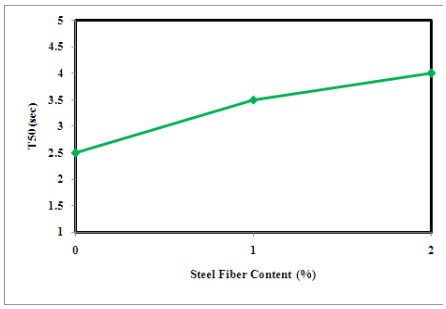

Figure 16: Effect of steel fiber content on T_{50} (sec) on normal SCC concrete.

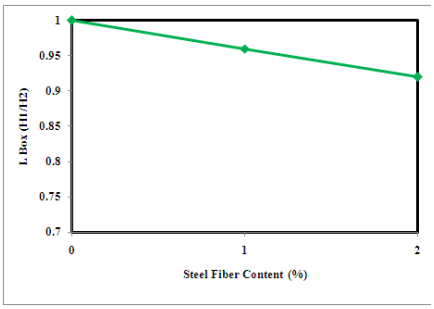

Figure 17: Effect of steel fiber content on L-Box on normal SCC concrete.

Preparation of Samples, Mixing, Casting and Curing

Mixing of concrete in a proper way leading to homogenous concrete and more strength is the main factors in any project. Various types of molds (wooden and steel) are used in this investigation for casting cylinders, cubes, prism, and columns with different concrete mixes of different grade. Firstly, cleaning and brush the mold form residual concrete and joining all molds parts, oiling the all internal sides and finally for casting of columns, steel reinforcing bars are arranged inside the mold in the correct position and fastened. Mixing was performed using laboratory horizontal mixer and performed according to [ASTM C305-99] limits. For normal self-compacted concrete, mixing was accomplished in a classical procedure where the coarse aggregates (gravel and sand) were mixed firstly, then cement was added to the mixer and mixed for sufficient time, finally, water combined with superplasticizer introduced into the mixer until obtaining a homogeneous mixture. For high and ultra-high self-compacted concrete, the fine materials (cement and silica fume) mixed firstly, then joining the sand and mixed for sufficient time. Superplasticizer is mixed with water producing aqueous solution applied to the dry mix.

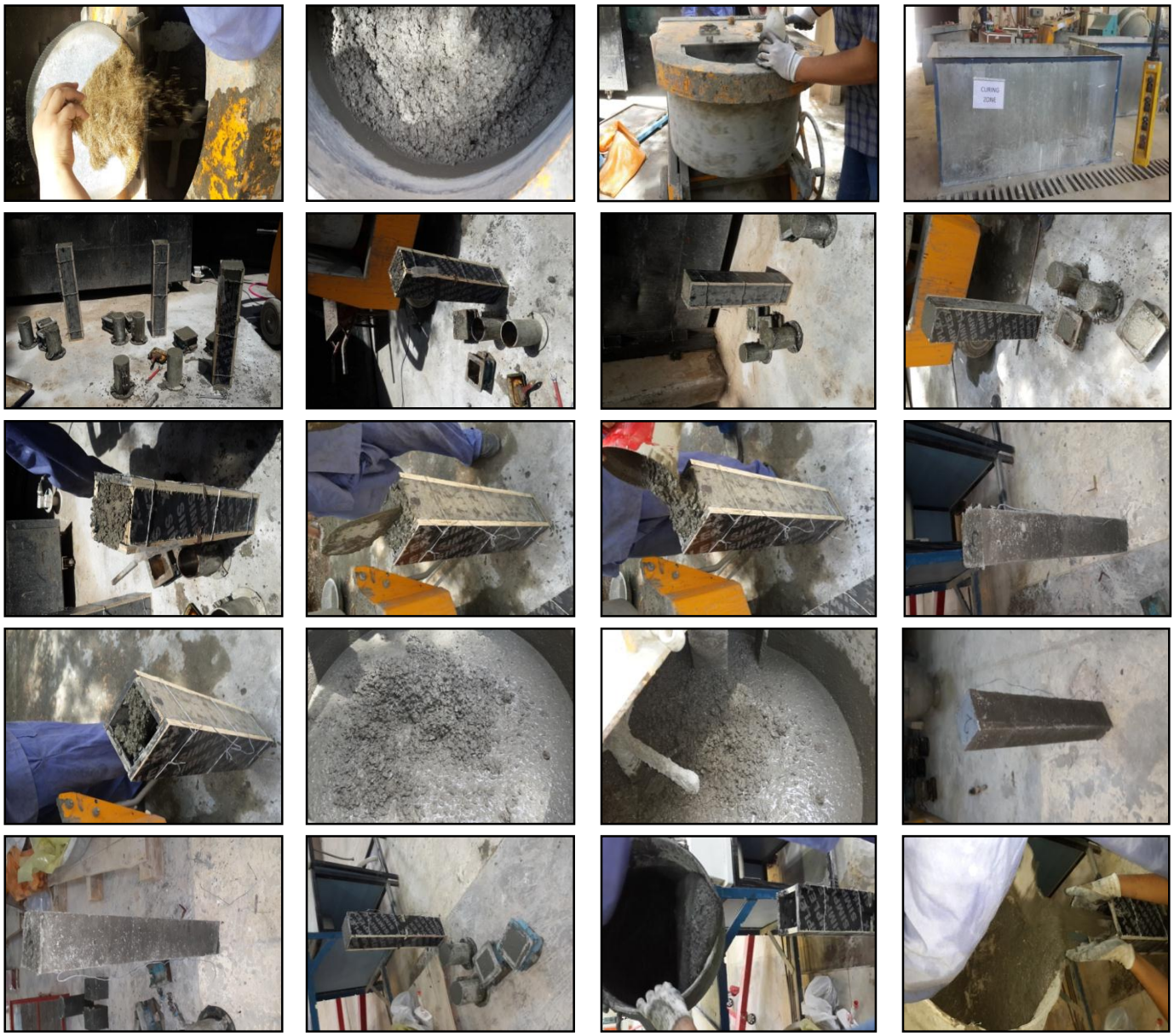

Figure 18: Preparation, mixing, casting and curing procedure.

A concrete mixture that having steel fiber, it introduced into the mixer by distribution by hand to prevent gathering by attraction. Mixing is done when a homogenous solution is concluded. After completing the mixing process, it is time for casting the molds where cylinders and column are cast in three layers while cubes and prisms in two layers all the layer should have appropriate and sufficient mixing. After completing the casting all molds should be covered to prevent the hydration water from evaporation and producing shrinkage in concrete. After one day all molds are opened and the specimens transformed to the curing tanks for 28 days, in the end, the specimens uploaded form the tanks waiting for testing time.

Figure 18: continued.

Table 13: Properties of hardened concrete and increasing percentage.

Mix	Steel fiber (%)	f'c (MPa)	(%) Increase in Compressive Strength	f_r (MPa)	(%) Increase in Flexural Strength	f_t (MPa)	(%) Increase in Splitting Tensile Strength	E_c (MPa)	(%) Increase in Modulus of Elasticity Strength
UHSC-SCC	0%	95	0	13	0	12	0	44.8	0
UHSC–SCC	1%	115	21.05	15	15.38	13	8.33	48	7.14
UHSC-SCC	2%	125	31.58	17	30.77	15	25	50	11.61
HS-SC	0%	50	0	6.66	0	6.2	0	33	0
HS-SC	1%	60	20	7.31	9.76	6.8	9.68	36	9.09
HS-SC	2%	70	40	7.69	15.47	7.4	19.35	39	18.18
N-SC	0%	30	0	4.4	0	4.21	0	25	0
N-SC	1%	35	16.67	5.2	18.18	4.8	14.01	27	8
N-SC	2%	39	30	5.8	31.82	5.2	23.52	31	24

Mechanical Properties of Hardened Concrete

Table (13) shows the hardening properties details of mixes used in the present research.

Compressive Strength

According to [ASTM C39-2005] specifications and applying (100x200 mm cylindrical specimens), the concrete compressive strength was determined to apply a hydraulic digital compression device (ELE-Digital Elect).

1-For Ultra-High SCC Concrete:

Three steel fiber ratios were chosen to study its effects on compressive strength. When steel fiber increase from (0, 1.0 and 2.0%) an increase of about (0, 21.05 and 31.58%) was achieved, as shown in Figure (19).

1-For High SCC Concrete:

Three steel fiber ratios were chosen to study its effects on compressive strength. When steel fiber increase from (0, 1.0 and 2.0%) an increase of about (0, 20 and 40%) was achieved, as shown in Figure (20).

1-For Normal SCC Concrete:

Three steel fiber ratios were chosen to study its effects on compressive strength. When steel fiber increase from (0, 1.0 and 2.0%) an increase of about (0, 16.67 and 30%) was achieved, as shown in Figure (21).

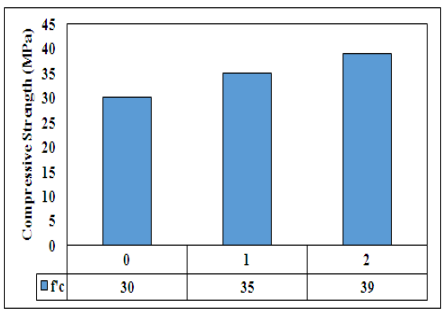

Figure 19: Effect of steel fiber on compressive strength of ultra-high strength SCC concrete.

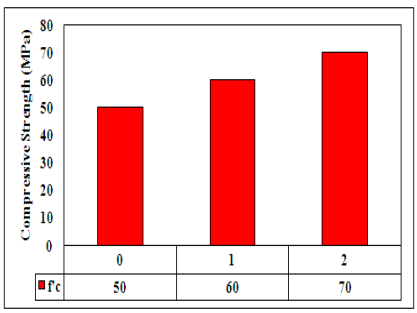

Figure 20: Effect of steel fiber on compressive strength of high strength SCC concrete.

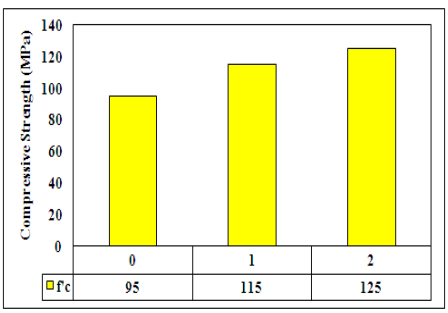

Figure 21: Effect of steel fiber on compressive strength of normal SCC concrete.

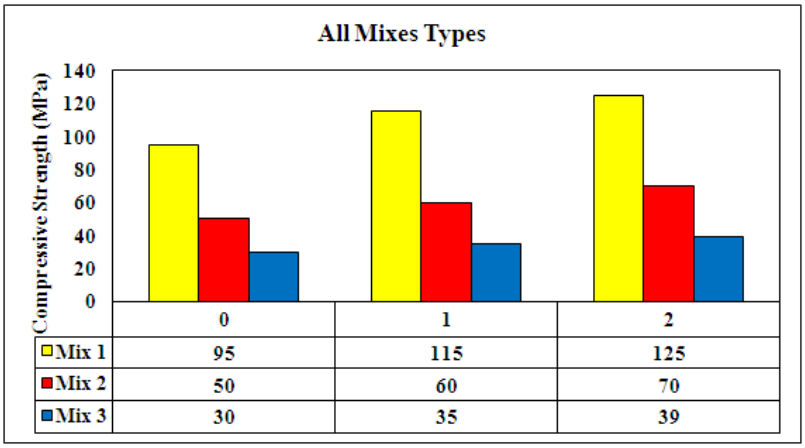

Flexural Strength Test

According to [ASTM C348-02] specifications and applying (70×70×280mm concrete prisms), the concrete flexural strength with two-point loading was determined to apply (ELE) digital electric testing device. The test concluded that the joining of steel fibers to concrete mix leads to better characteristics and enhanced concrete in bending and minimizing the differences in sizes of concrete components (grain size) leads to reduce pore size which strengthens the transition zone at the interface and reduce all cracking size.

1-For Ultra-High SCC Concrete:

Three steel fiber ratios were chosen to study its effects on flexural strength. When steel fiber increase from (0, 1.0 and 2.0%) an increase of about (0, 15.38 and 30.77%) was achieved, as shown in Figure (22).

1-For High SCC Concrete:

Three steel fiber ratios were chosen to study its effects on flexural strength. When steel fiber increase from (0, 1.0 and 2.0%) an increase of about (0, 9.76 and 15.47%) was achieved, as shown in Figure (23).

1-For Normal SCC Concrete:

Three steel fiber ratios were chosen to study its effects on flexural strength. When steel fiber increase from (0, 1.0 and 2.0%) an increase of about (0, 18.18 and 31.82%) was achieved, as shown in Figure (24).

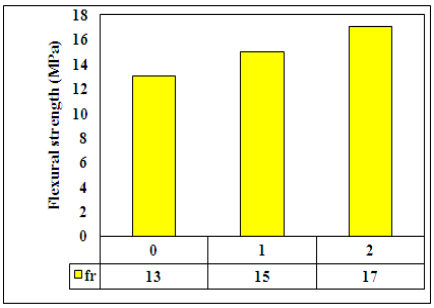

Figure 22: Effect of steel fiber on flexural strength of ultra-high strength SCC concrete.

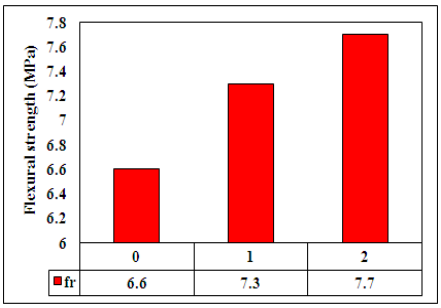

Figure 23: Effect of steel fiber on flexural strength of high strength SCC concrete.

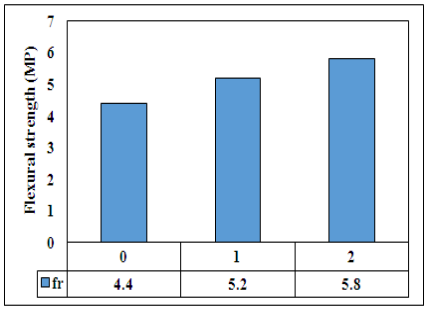

Figure 24: Effect of steel fiber on flexural strength of normal SCC concrete.

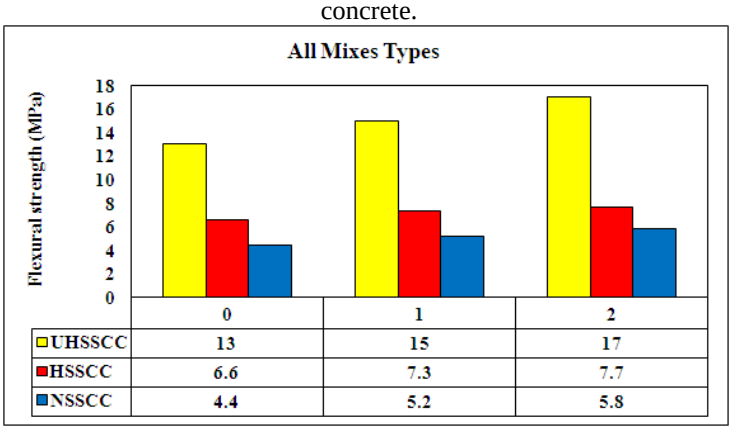

Splitting Tensile Strength Test

Testing was performed using a digital testing (ELE-Digital Elect 2000) to measure splitting tensile strength through cylinders of (100×200mm) accordance [***ASTM specification C496-04***]. The test concluded that fibers improve the physical, characteristic and concrete matrix within the hardening state. Fiber has the ability to work as a crack reducer through capturing of crack or as cracks arrestor which bridge the cracks and transformed stresses from one side to another across a crack.

1-For Ultra-High SCC Concrete:

Three steel fiber ratios were chosen to study its effects on splitting tensile strength. When steel fiber increase from (0, 1.0 and 2.0%) an increase of about (0, 8.33 and 25%) was achieved, as shown in Figure (25).

1-For High SCC Concrete:

Three steel fiber ratios were chosen to study its effects on splitting tensile strength. When steel fiber increase from (0, 1.0 and 2.0%) an increase of about (0, 9.68 and 19.35%) was achieved, as shown in Figure (26).

1-For Normal SCC Concrete:

Three steel fiber ratios were chosen to study its effects on splitting tensile strength. When steel fiber increase from (0, 1.0 and 2.0%) an increase of about (0, 14.01 and 23.52%) was achieved, as shown in Figure (27).

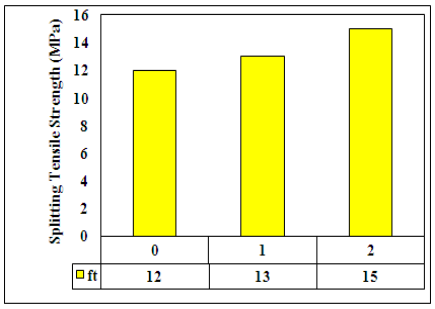

Figure 25: Effect of steel fiber on splitting tensile strength of ultra-high strength SCC concrete.

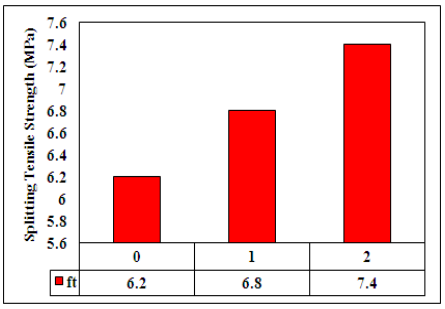

Figure 26: Effect of steel fiber on splitting tensile strength of high strength SCC concrete.

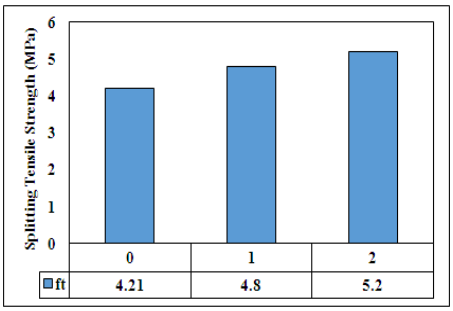

Figure 27: Effect of steel fiber on splitting tensile strength of normal SCC concrete.

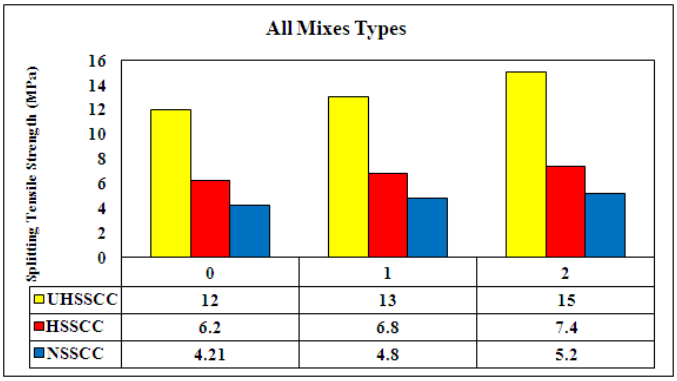

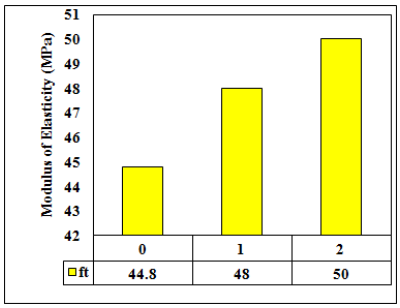

Figure 28: Effect of steel fiber on modulus of elasticity of ultra-high strength SCC concrete.

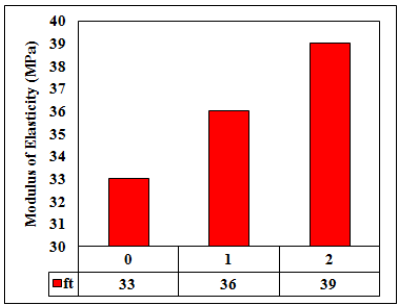

Figure 29: Effect of steel fiber on modulus of elasticity of high strength SCC concrete.

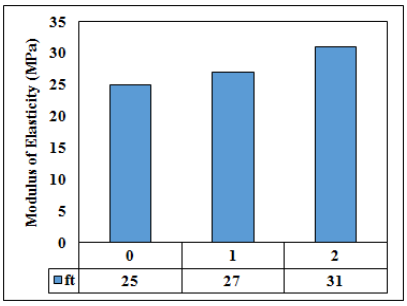

Figure 30: Effect of steel fiber on modulus of elasticity of normal SCC concrete.

Figure 31: compressive strength, splitting tensile strength, and modulus of rupture tests.

Modulus of Elasticity

According to [ASTM C469-02] specifications and limitations, the modulus of elasticity test was experimentally performed to show the slopes and strength of materials.

1-For Ultra-High SCC Concrete:

Three steel fiber ratios were chosen to study its effects on the modulus of elasticity. When steel fiber increase from (0, 1.0 and 2.0%) an increase of about (0, 7.14 and 11.61%) was achieved, as shown in Figure (28).

1-For High SCC Concrete:

Three steel fiber ratios were chosen to study its effects on the modulus of elasticity. When steel fiber increase from (0, 1.0 and 2.0%) an increase of about (0, 9.09 and 18.18%) was achieved, as shown in Figure (29).

1-For Normal SCC Concrete:

Three steel fiber ratios were chosen to study its effects on the modulus of elasticity. When steel fiber increase from (0, 1.0 and 2.0%) an increase of about (0, 8 and 24%) was achieved, as shown in Figure (30).

Testing Procedure

Reinforced concrete columns casting from of all types of concrete mixtures were examined in a loading device with a capacity of (3000 kN). Before starting the examination, there are some procedures to be taken. First, remove the specimens from the treatment containers and then wait for drying. Then clean it with the brush and expose it to the white painting for easy examination and draw the cracks and to be photographed before and after the start of the examination. Then prepare all the requirements for each test. The column is loaded and placed on the loading device vertically. Before the start of the loading process, pieces of rubber shall be placed on top and bottom of the model to ensure that the concrete is not crushed. After that, the forces shall be applied to the column in small divided steps to ensure that the column does not fail from the beginning and that these loads should be placed vertically and centrally. At the start of the test and operation of the device, the device is connected to an external electronic computer to record all loads and axial deformation to give full calculations and sufficient to draw load-deflection curve. During the loading process and during the appearance of cracks on the surface of the concrete, the column must be marked, this marked shows reading loads and cracks on the concrete surface of the column. Loading is continued until the column fails where the device stops recording.

Mode of Failure

Photographs of the tested columns with the mode of failure and crack pattern before and after testing are shown in Figure (32). The cracks were generated in the concrete when the tensile stress reaches its strength limit. At the testing time, for the non-fibrous concrete, most of the column specimens produced very similar behavior at early loading stages and the column deformations produced were initially at the elastic zone, and

then the applied load was increased until the first crack occurred. As the load increased further, cracks developed and they increased in depth. At the final loading stage, the concrete cover at compression side was crushing and spalling and the specimens were buckled to the outside and at the end, the column failed by yielding of longitudinal steel reinforcement. For fibrous concrete column this behavior is not noticed, where the steel fiber is the primary factor that affects the appearance of cracks in concrete and changed the mode of failure from brittle to ductile. Increasing steel fiber generated more strength columns with higher ultimate loads and lesser deformation and with improvements in ductility and toughness. The increasing grade of concrete from normal to high and ultra-high strength changed the columns behavior to better performance and higher strength. The contribution of fiber and their excellent orientation and distribution in the mixture prevents of the appearance of crack and reduces the tensile stress at the cracks zone which restricted the cracking propagation.

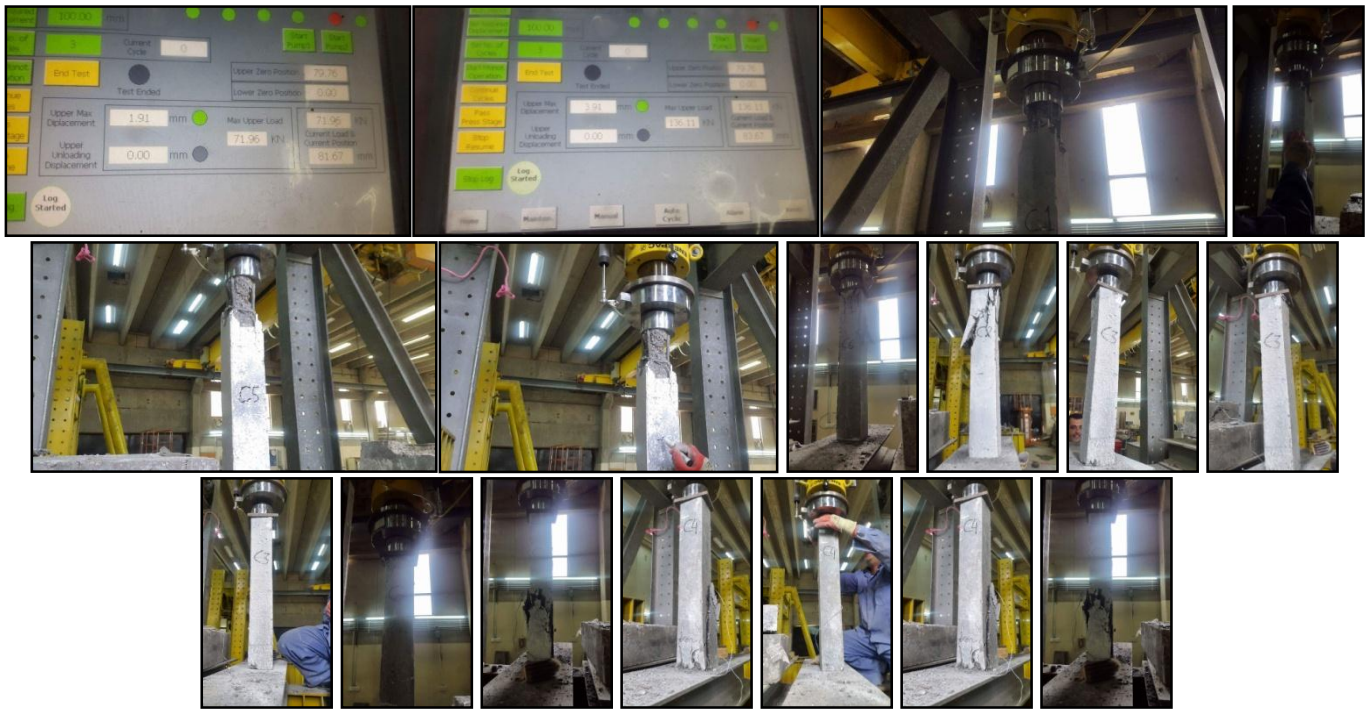

Figure 32: Test setup, crack pattern and mode of failure columns.

Ultimate Capacity and Load-Displacement

The tested columns were divided into three groups: the first group consists of (ultra-high strength self-compacting concrete with 3 steel fiber ratios), the second group (high strength self-compacting concrete with 3 steel fiber ratios). The third group ((Normal self-compacting concrete with 3 steel fiber ratios). The failure loads of all columns specimen are shown in the table (14). By distinguishing between the varieties of concrete, it can be remarked that the ultra-high strength SCC columns are the toughest collection according to the ultimate carrying load and next attains the high and finally the normal SCC group. This may be related to the composition of mixes and the presence of steel fibers in concrete advance its properties, particularly the compressive strength. For group (1), when steel fiber added the failure load was indicating a significant enhancement in the ultimate capacity of about (0, 17.73 and 26.67%) as shown in Figure (33). For group (2), during steel fiber combined the failure load was indicating a significant intensification in the ultimate capacity of about (0, 14.29 and 30.95%) as shown in Figure (34). For group (3), when steel fiber joined the failure load was showing an important enhancement in the ultimate capacity of about (0, 10.34 and 20.69%) as shown in Figure (35). At initial stages of loading, the column deformations obtained initially within the linear scales, and later the implemented load was developed continuously the first crack happened. The cracks width progressed before the peak load reached. The second stage is the non-elastic performance of the load-deflection description, the material functions inelastically in tension and however elastic in compression and the cracks are admitted at the utmost fiber of the segment and propagated approaching the interior fibers. Improvement in the load carrying capacity beyond the proportionate boundary is related to a consecutive elevation in the location of the neutral axis approaching the compression region, while the concentration of tensile bending stress at the cracked fibers of the section continues further or less uniform and equivalent to the highest post cracking stress of the substance. Figure (36, 37 and 38) show effect of steel fiber content ratio on a load-deflection curve. However, columns with steel fibers inclusion declared a ductile achievement, while columns without fiber exhibited a brittle response due to the active expansion of cracks. From the load-deflection relation given in this study, it was apparent that the steel fiber columns displayed greater load than non-fibrous columns.

Furthermore, it can be remarked that an increase in ductility was produced for specimens due to the inclusion of the steel fibers. These behaviors can be illustrated, throughout the using of high ratios of small steel fibers concurrently with the valid bond connecting fiber and matrix and this leads to an improvement in tensile cracking which offered high endurance to fiber pull out and considerably enhance the toughness of the material.

Table 14: Effect of steel fiber content ratio (%) on load deflection curve.

Mix	Dimension (mm)	Longitudinal steel bars	Tie bars	Ultimate load (kN)	Percentage Increase in ultimate load (%)	Axial deformation (mm)
UHSC-SCC	100*100*700	4-φ10	4-φ4	705	0.00	6.78
UHSC–SCC	100*100*700	4-φ10	4-φ4	830	17.73	8
UHSC-SCC	100*100*700	4-φ10	4-φ4	893	26.67	9.05
HS-SC	100*100*700	4-φ10	4-φ4	420	0.00	5.2
HS-SC	100*100*700	4-φ10	4-φ4	480	14.29	5.6
HS-SC	100*100*700	4-φ10	4-φ4	550	30.95	6.2
N-SC	100*100*700	4-φ10	4-φ4	290	0.00	4.7
N-SC	100*100*700	4-φ10	4-φ4	320	10.34	5
N-SC	100*100*700	4-φ10	4-φ4	350	20.69	5.2

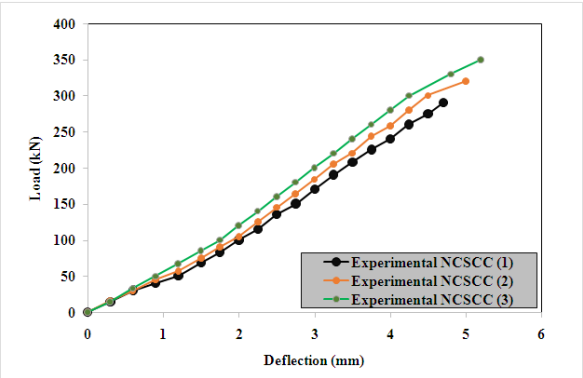

Figure 33: Load-deflection curve for NCSCC columns (1, 2 and 3).

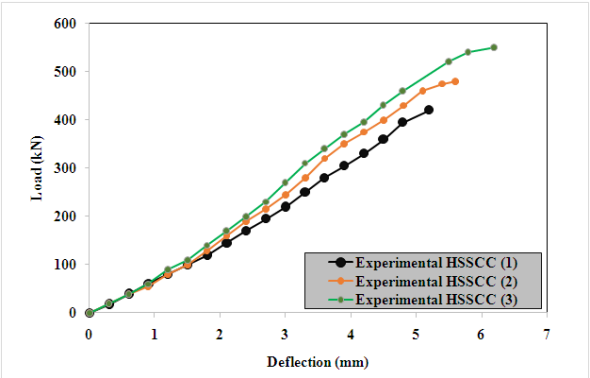

Figure 34: Load-deflection curve for HSSCC columns (1, 2 and 3).

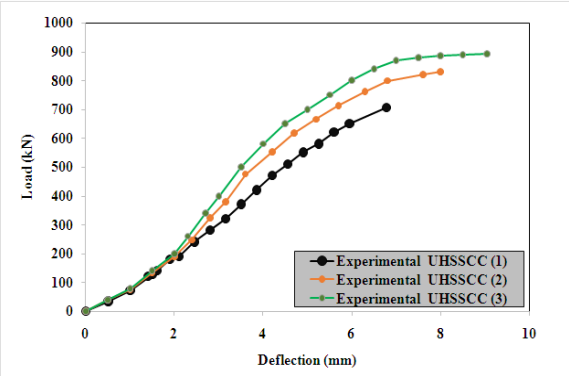

Figure 35: Load-deflection curve for UHSSCC columns (1, 2 and 3).

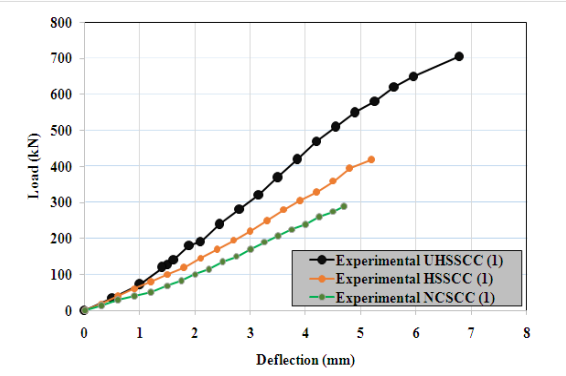

Figure 36: Comparison between (NCSCC, HSSCC and HSSCC Load-deflection curve (steel fiber 0%).

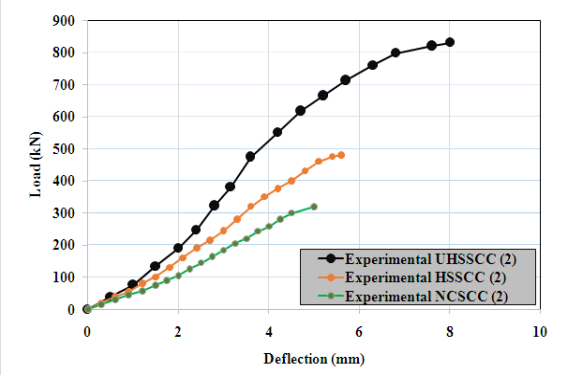

Figure 37: Comparison between (NCSCC, HSSCC and HSSCC Load-deflection curve (steel fiber 1.0%).

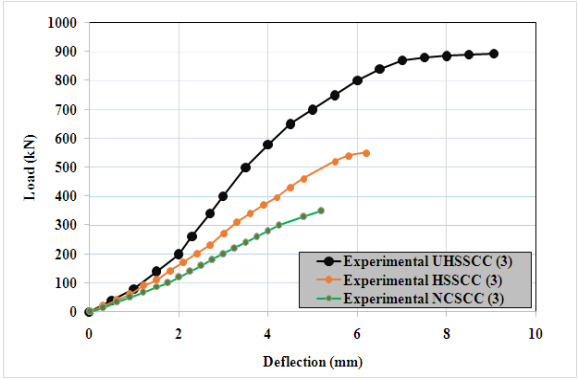

Figure 38: Comparison between (NCSCC, HSSCC and HSSCC Load-deflection curve (steel fiber 2.0%).

NON-LINEAR Finite Element Modeling of Test Specimens

Experimental tests are generally used as a test method to analyze individual elements in order to achieve an acceptable precision for practical use. But these types of test produce a response in real life is time-consuming, and the use of materials can be quite expensive. The applications of finite element analysis have been improved due to the development of concrete technology and structures and the simplicity of using of computer software. The finite element method becomes the method of choice to analyze concrete structural components since it is much faster and extremely profitable. The non-linear finite element analysis was transported to investigate the behavior of the reinforced concrete columns using the ANSYS software. The investigated behavior includes the crack pattern, the maximum load and the load and deflection response of the columns. An acceptable concordance was found between the experimental tests conclusions and the finite element program.

Geometry Modeling

In this study, nine columns were analyzed by ANSYS programs. The FEA study includes the modeling of normal, high and ultra-high-strength reinforced concrete column, with the dimensions and properties corresponding to the actual experimental data. The specimen will be modeled using eight-node three-dimensional concrete solid element (SOLID65) and (link8) element was used to model the steel reinforcement, with two nodes to represents the link element, with 3 degrees of freedom and translations in x, y, and z directions. The comparison shows that the ANSYS nonlinear finite element program is capable of modeling and predicting the actual nonlinear behavior of columns with having different characteristics. (28) show solid 65 and 3D-LINK 8 for concrete and steel.

Material Properties (Concrete)

To represent the differences in materials in the program a stress-strain diagram must be introduced. Concrete has two stress-strain drawing depends on the behavior of concrete in compression and tension. The concrete stress-strain concluded from experimental work of cylinders in compression state test. Division of the curve into multiple points with x and y coordinate data to represent the curve through the program must be applied from the beginning of the curve through the ultimate compressive strength till the crushing on concrete as shown in Figure (40). The small division must be performed to represent the whole curve.

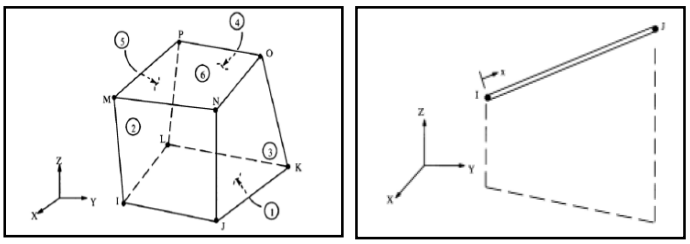

Figure 39: Solid 65 and 3D-LINK 8 for concrete and steel.

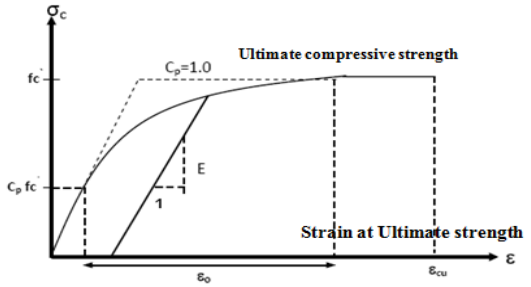

Figure 40: Compression uniaxial stress-strain curve for concrete in compression.

Behavior of Concrete in Tension (Behavior of steel fiber reinforced concrete)

Concrete is simulated in tension by (tensile-stress-strain diagram), which can be presented and explained before cracking by linear elastic model. Generally, after concrete cracking; cracking could be presented by principal tensile stresses or strain which related to the beginnings of cracks appearance. To represent the tensile behavior, the theoretical work presented two methods of tension-stiffening model which are (TS1 and TS2 define as suitable for analyzing reinforced concrete sections without fibers and suitable for analyzing fiber reinforced concrete sections and has the ability to produce theoretical load-deflection response close to experimental one and the ultimate loads are close to the actual experimental failure loads. as shown in Figure (41), the reason for using tension-stiffing model and no other model because of concrete during cracking still holding a tensile stresses perpendicular to the cracks itself.

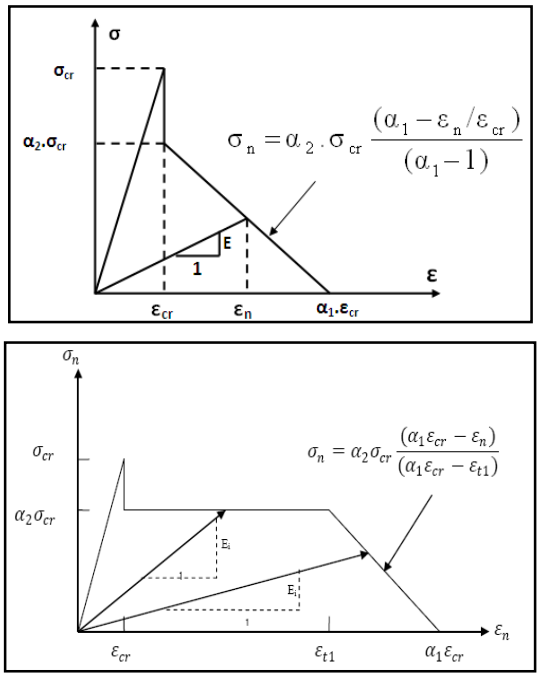

Figure 41: Post-cracking model of conventionally reinforced concrete and steel fiber reinforced concrete (TS1and TS2).

Element Meshing, Loads and Boundary conditions

After collecting all the data required to be entered into the program in terms of physical properties and engineering division and the size, dimensions and areas of reinforcing steel and concrete, initially insert the desired shape by applying it to the program and then get a whole general shape to be then divided into small elements into cubes to give and simulate the original shape of the column, which was examined by practical examination. All the data entered into the program correctly makes the program work and simulates the column theoretically in terms of the loads that can be applied to the column. Before the implementation of the analysis by the program, there are some requirements that must be met to ensure that the model works, these are the locations of loading and places of support where all movement in the bottom of the column held to zero (δx=0, δz=0, and δy=0). The movement of the column was stopped to parallel the non-movement of the device and the installation of the model. From the top, loads were placed, similar to loads carried from the device, but was divided and distributed on the nodes to represent the central axial pressure. Before running the program, the loads are divided into steps to prevent the failure of the model and theoretically assume these loads according to the Newton-Raphson procedure. The program runs in order to analyze and draw the relationships, which is the ultimate load. Then the program stops and the highest failure load was concluded. The solution is stopped for compatibility between the theoretical and practical solution. Failure of the theoretical model can be determined when the solution for a minimum load steps cannot be converging.

Analysis of Samples

Figures from (42-50) below show the comparison between the ultimate load-deflection curve of the experimentally tested column and finite element program. The theoretical work is applied to verify the finite element programs have the ability to examine many structural elements. The programs able to show the failure ultimate loads, cracking loads, deformations, mode of failure and stresses contour diagram, all these parameters work as ensuring factors for the accuracy of the finite element models compared to the experimental results. In the present investigation, the predicted load-deflection curve obtained are compatible with experimental load-deflection curve from the beginning of loading through cracking load finally till the ultimate load. After cracking load, a slight differences response is presented. At the final loading stage yielding of steel reinforcement followed by concrete, crushing is the failure type of column presented in this numerical research. It was concluded that the general behavior of the finite element models shows a proved compatibility with the experimental tests results between (87% to 95%). From the stresses contour, the plot shows that the concentration of higher axial stress presented within the center region of the cross-section for the column. Figure (51) show differences in ultimate load between three concrete types. Stresses contour of the finite element of the analyzed columns is shown in Figures (52).

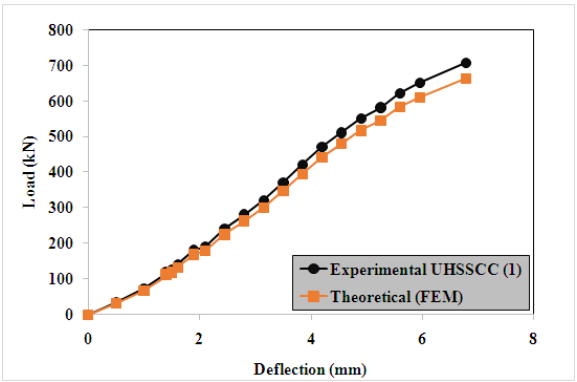

Figure 42: Comparison between EXP. and Ansys load-deflection curve for UHSSCC (1).

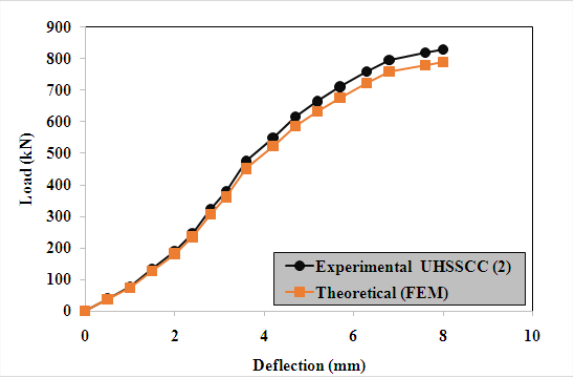

Figure 43: Comparison between EXP. and Ansys load-deflection curve for UHSSCC (2).

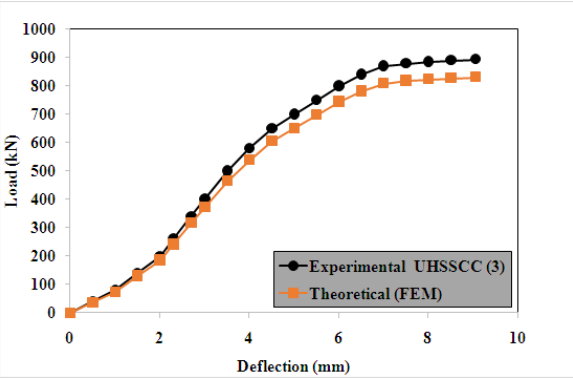

Figure 44: Comparison between EXP. and Ansys load-deflection curve for UHSSCC (3).

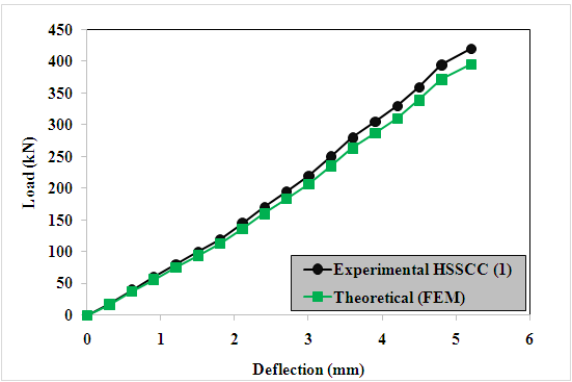

Figure 45: Comparison between EXP. and Ansys load-deflection curve for HSSCC (1).

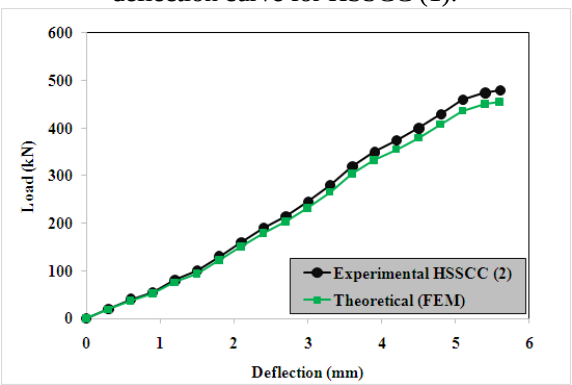

Figure 46: Comparison between EXP. and Ansys load-deflection curve for HSSCC (2).

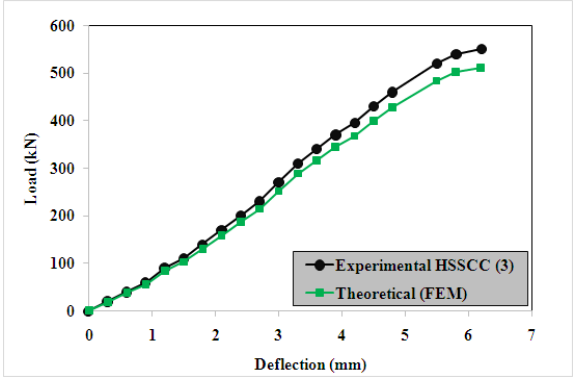

Figure 47: Comparison between EXP. and Ansys load-deflection curve for HSSCC (3).

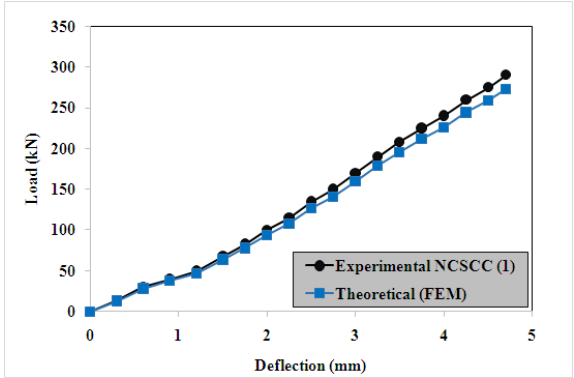

Figure 48: Comparison between EXP. and Ansys load-deflection curve for NCSCC (1).

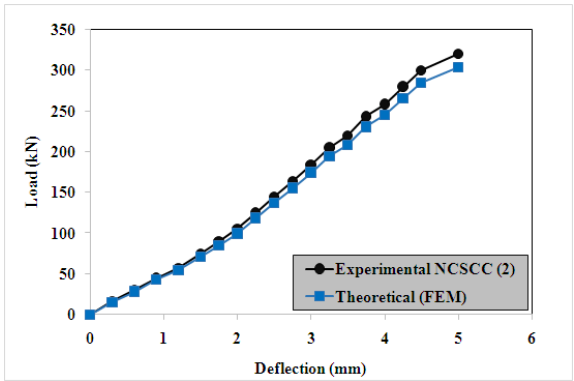

Figure 49: Comparison between EXP. and Ansys load-deflection curve for NCSCC (2).

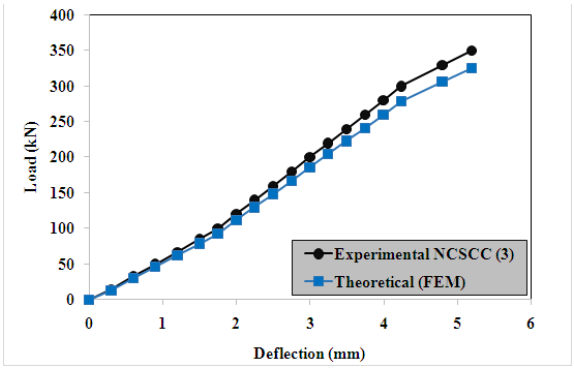

Figure 50: Comparison between EXP. and Ansys load-deflection curve for NCSCC (3).

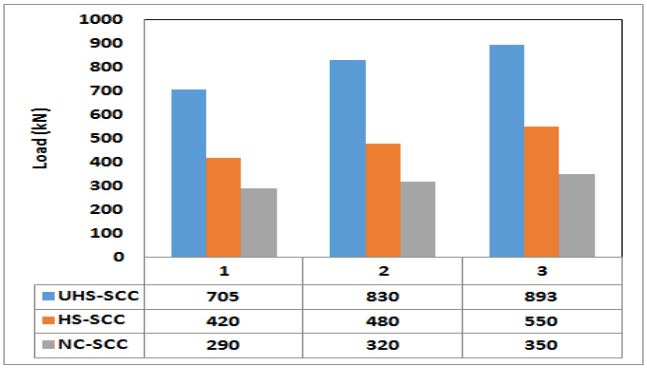

Figure 51: Differences in ultimate load between three concrete types.

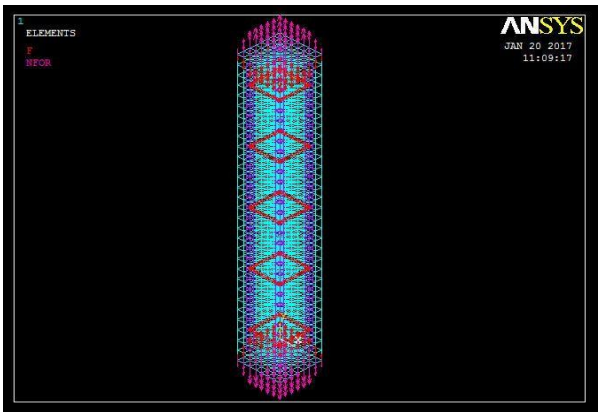

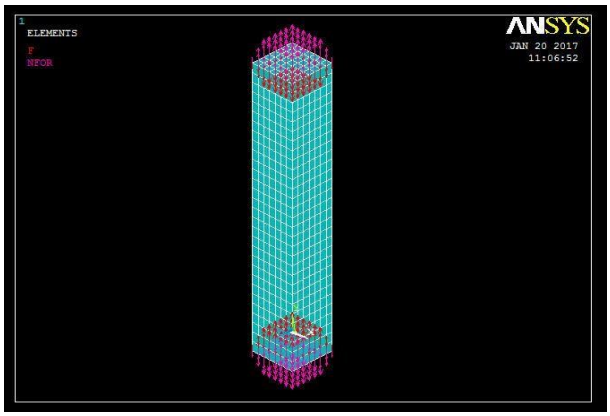

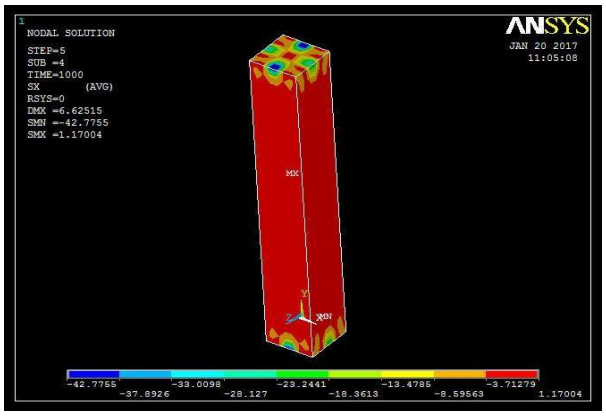

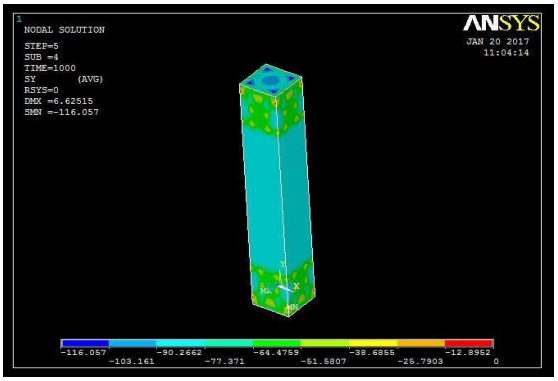

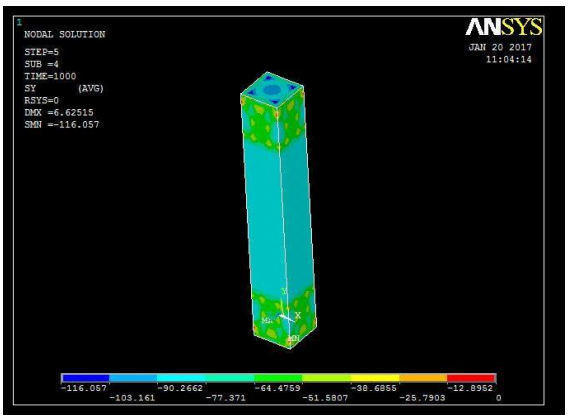

Figure 52: Modeling of specimens, boundary conditions, loadings, meshing and stress diagram.

Comparison of experimental ultimate load with codes Equations

When comparing the ultimate load obtained from the experimental test with codes equations and finite element program (Ansys) differences are appeared. A review of some codes equations is given here. Table (15) show codes equations and table (16) show a comparison between experimental ultimate load, codes equation and Ansys loads. The tables show that (ACI/EXP) relation is higher than (FEM/EXP) relation while (B.S./EXP) and (CAN/EXP) relation give much lower than (FEM/EXP). That means that FEM program (Ansys) was able to predict close results compared to experimental work within ultimate load and behaviors.

Table 15: Codes equations for predicting axial column capacity.

Code	Equation	Where:
ACI-318M-08 code	$P_n=0.85*f'_c*A_n+f_y*A_{st}$	A_n (mm^2)=concrete net area $=A_g-A_{st}$
B.S 8110-97 code	$P_n=0.4*f'_{cu}*A_n+0.75*f_y*A_{st}$	
Canadian code-1984	$P_n=0.51*f'_c*A_n+0.85f_y*A_{st}$	

Table 16: Comparison between experimental ultimate load, codes equation and Ansys.

Mix	Exp. load (kN)	FEM. load (kN)	FEM/EXP	ACI	ACI /EXP	B.S.	B.S./EXP	Canadian	Can/EXP
UHSCSCC	**705**	**662.7**	**0.94**	**942.9**	**1.34**	**488.6**	**0.69**	**605.9**	**0.86**
UHSCSCC	**830**	**788.5**	**0.95**	**1107.6**	**1.33**	**566.1**	**0.68**	**704.7**	**0.85**
UHSCSCC	**893**	**830.5**	**0.93**	**1189.9**	**1.33**	**604.9**	**0.68**	**754.1**	**0.84**
HS-SC	**420**	**394.8**	**0.94**	**572.4**	**1.36**	**314.3**	**0.75**	**383.6**	**0.91**
HS-SC	**480**	**456.0**	**0.95**	**654.8**	**1.36**	**353.0**	**0.74**	**433.0**	**0.90**
HS-SC	**550**	**511.5**	**0.93**	**737.1**	**1.34**	**391.8**	**0.71**	**482.4**	**0.88**
N-SC	**290**	**272.6**	**0.94**	**407.8**	**1.41**	**236.8**	**0.82**	**284.8**	**0.98**
N-SC	**320**	**304.0**	**0.95**	**448.9**	**1.40**	**256.2**	**0.80**	**309.5**	**0.97**
N-SC	**350**	**325.5**	**0.93**	**481.9**	**1.38**	**271.7**	**0.78**	**329.3**	**0.94**

CONCLUSIONS

1. Three concrete types (normal, high and ultra-high self-compacting concrete) are presented in term of reinforced concrete column through experimental and theoretical work.
2. Steel fiber effects with ratios of (0, 1 and 2%) were study on ultimate capacity, mode of failure, cracking and the deformation behavior for the three concrete types.
3. Self-compacted concrete with higher grade is much better in fresh and hardened properties compared to others and increase the performance of columns through strength, toughness, workability, ultimate load, reduction in cracking and ductility.
4. Increasing of fiber from (0 to 1 and 2%) decreases the slump by [(10.7% and 22.7%), (3.8% and 7.7%), (9.3% and 13.3%)] increasing T_{50} [(49.5% and114.3%), (16% and 36%), (40% and 60%)] reduction L-box by [(9.3% and 17.5 %), (5.1% and 10.2 %), (4% and 8%)] for ultra-high SCC, high SCC and normal SCC respectively. Fiber works as an obstacle for the motion and reduce the workability.
5. Increasing of fiber from (0 to 1 and 2%) cause an increase in compressive strength of about [(0, 21.05 and 31.58%), (0, 20 and 40%), (0, 16.67 and 30%)] for ultra-high SCC, high SCC and normal SCC respectively.
6. Increasing of fiber from (0 to 1 and 2%) cause an increase in flexural strength of about [(0, 15.38 and 30.77%), (0, 9.76 and 15.47%), (0, 18.18 and 31.82%)] for ultra-high SCC, high SCC and normal SCC respectively. Fibers reduce the cracks width by reducing the stresses concentrations.
7. Increasing of fiber from (0 to 1 and 2%) cause an increase in splitting tensile strength of about [(0, 8.33 and 25%), (0, 9.68 and 19.35%), (0, 14.01 and 23.52%)] for ultra-high SCC, high SCC and normal SCC respectively. Fibers reduce the cracks width by reducing the stresses concentrations.
8. Increasing of fiber from (0 to 1 and 2%) cause an increase in modulus of elasticity of about [(0, 7.14 and 11.61%), (0, 9.09 and 18.18%), (0, 8 and 24%)] for ultra-high SCC, high SCC and normal SCC respectively. Fibers reduce the cracks width by reducing the stresses concentrations.
9. The compatibility between the experimental tests results and theoretical analysis are between (87% to 95%).

REFERENCES

[1] Al-Shamma Y. M. “Strength and Ductility of Confined Steel Fiber Reinforced Concrete Short Columns”, MSc. Structural Engineering, Al-Mustansiriya University, Baghdad, 113 pp, (2011).

[2] Malik, Adnan R., Foster Stephen J. “Behavior of Reactive Powder Concrete Columns without Steel Ties”, Journal of advanced concrete technology, Vol. 6, No. 2, PP.377-386, (2008).

[3] Grunewabl, S. “Performance Based Design of Self Compacting Fiber Reinforced Concrete”, Ph.D. Thesis, Delft University of Technology, Netherlands, pp. 165, (2004).

[4] Ganesan N., Indira P.V., and Santhosh Kumar P.T. “Strength and Behavior of Steel Fiber Reinforced Self Compacting Concrete in Flexure”, Proceedings of the International Conference on Advanced in Concrete

composites and Structures, SERC, Chennai, (2005).

[5] Steffen G. and Joost C. W. "Transporting Fibers as Reinforcement in Self-Compacting Concrete", University of Technology, the Netherlands, pp100-125, (2009).

[6] Holschemacher, K., and Klug, Y. "A Database for the Evaluation of Hardened Properties of Self-Compacting Concrete", LACER No.7, pp.123-134, (2002).

[7] Sonebi , M. , Grünewald , S., and Walraven , J. "Filling Ability and Passing Ability of Self-Consolidating Concrete" , ACI Materials Journal , Vol. 104, No. 2, March-April , pp.162-170, (2007).

[8] Grunewald, S. and Walraven, J.C. "Parameter Study on the Influence of Steel Fiber and Coarse Aggregate Content on the Fresh Properties of Self-Compacting Concrete" Cement and Concrete Research, Vol. 131, No. 12, pp.1793-1798, (2001).

[9] Suksawang, N., Nassif, H., Najm, S. "Evaluation of Mechanical Properties for Self-Consolidating, Normal, and High-Performance Concrete (HPC)", New Jersey Department of Transportation (NJDOT) and the Center for Advanced Infrastructure and Transportation (CAIT) at Rutgers, pp.3, (2006).

[10] Ferrara, L., Park, T.D. and Shah, S.P. "A Method for Mix-Design of Fiber Reinforced Self Compacting Concrete", Cement and Concrete Research, Vol.37, No. 6, PP. 957-971, 2007, (2007).

[11] Nehdi, M. and Ladanchnk, J.D. "Fiber Synergy in Fiber Reinforced Self-Consolidating Concrete", ACI Material Journal, Vol.101, No.6, pp. 508-517, (2004).

[12] Heba A. Mohamed. "Effect of fly ash and silica fume on compressive strength of self-compacting concrete under different curing conditions", Ain Shams Engineering Journal, Vol.2, pp.79-86, (2011).

[13] MuctebaUysal "Self-compacting concrete incorporating filler additives: Performance at high temperatures", Construction and Building Materials, Vol.26, No. 1, pp.701-706, (2012).

[14] Xie Y., Liu B., Yin J. and Zhou S. "Optimum mix parameters of high-strength self-compacting concrete with ultrapulverised fly ash", Cem. Concr. Res, Vol.32, No.3, pp.477-80, (2002).

[15] Foster, S. J. and Attard, M. M. "Strength and Ductility of Fiber-Reinforced High-Strength Concrete Columns", Journal of Structural Engineering, ASCE, Vol.127, No. 1, pp. 28-34, (2001).

[16] Efe E. I. and Musbau A. S. "Effect of Short Steel Fiber Reinforcement on Laterized Concrete Columns", Faculty of Engineering, University of Lagos Akoka, Yaba, Lagos, Nigeria, ACI Structural Journal, Vol. 4, No. 1, (2011).

[17] Hadi. M.N.S. "Reinforcing Concrete Columns with Steel Fibers", School of Civil and Environmental Engineering, University of Wollongong, Asian Journal of Civil Engineering (building and housing) V. 10, No. 1 pp 79-95, (2009).

[18] Campion, G., Fosseti, M., Papio M. "Behavior of Fiber-Reinforced Concrete Columns under axially and Eccentricity Compressive Loading", ACI Structural Journal, Vol. 107, No. 3, pp.272-281, (2010).

[19] Maha, M.S., Taghreed, K., and Zeena, W. "Behavior of Axially Loaded Reactive Powder Concrete Columns", Journal of Engineering and Development, Vol.17, No.2, (2013).